
Take A Shortcut Back: Mitigating the Gradient Vanishing for Training Spiking Neural Networks

Yafei Guo*, **Yuanpei Chen***
 Intelligent Science & Technology Academy of CASIC
 yfguo@pku.edu.cn

Abstract

The Spiking Neural Network (SNN) is a biologically inspired neural network infrastructure that has recently garnered significant attention. It utilizes binary spike activations to transmit information, thereby replacing multiplications with additions and resulting in high energy efficiency. However, training an SNN directly poses a challenge due to the undefined gradient of the firing spike process. Although prior works have employed various surrogate gradient training methods that use an alternative function to replace the firing process during back-propagation, these approaches ignore an intrinsic problem: gradient vanishing. To address this issue, we propose a shortcut back-propagation method in our paper, which advocates for transmitting the gradient directly from the loss to the shallow layers. This enables us to present the gradient to the shallow layers directly, thereby significantly mitigating the gradient vanishing problem. Additionally, this method does not introduce any burden during the inference phase. To strike a balance between final accuracy and ease of training, we also propose an evolutionary training framework and implement it by inducing a balance coefficient that dynamically changes with the training epoch, which further improves the network's performance. Extensive experiments conducted over static and dynamic datasets using several popular network structures reveal that our method consistently outperforms state-of-the-art methods.

1 Introduction

Nowadays, the Spiking Neural Network (SNN), as one of the efficient neural networks has received a lot of interest and been widely used in many fields, *e.g.*, object recognition [32; 50], object detection [27; 40], pose tracking [57], and so on. The SNN utilizes the binary spike signals to transmit the information that when the membrane potential exceeds the threshold, the spiking neuron will fire a spike represented by 1, otherwise fire nothing represented by 0. The special information processing paradigm enjoys low energy consumption since it would convert multiplications of weights and activations to simple additions. Moreover, this information processing paradigm can be further implemented in a highly efficient event-driven-based computation manner on neuromorphic hardwares [35; 1; 7; 39], where the computational unit would be activated only when a spike comes, otherwise, will keep silent for save energy. It is shown that an SNN can save orders of magnitude energy over its Artificial Neural Network (ANN) counterpart [1; 7].

Despite the energy efficiency, it is difficult to train an SNN directly since the gradient of the firing spike process is not well-defined, which makes it impossible to train an SNN directly by gradient-based optimization methods. To solve this problem, various surrogate gradient training (SG) methods have been proposed [11; 41; 48; 37]. This kind of method uses an alternative function to replace the firing process when doing back-propagation. For example, the truncated quadratic function, the

*Equal Contributions.

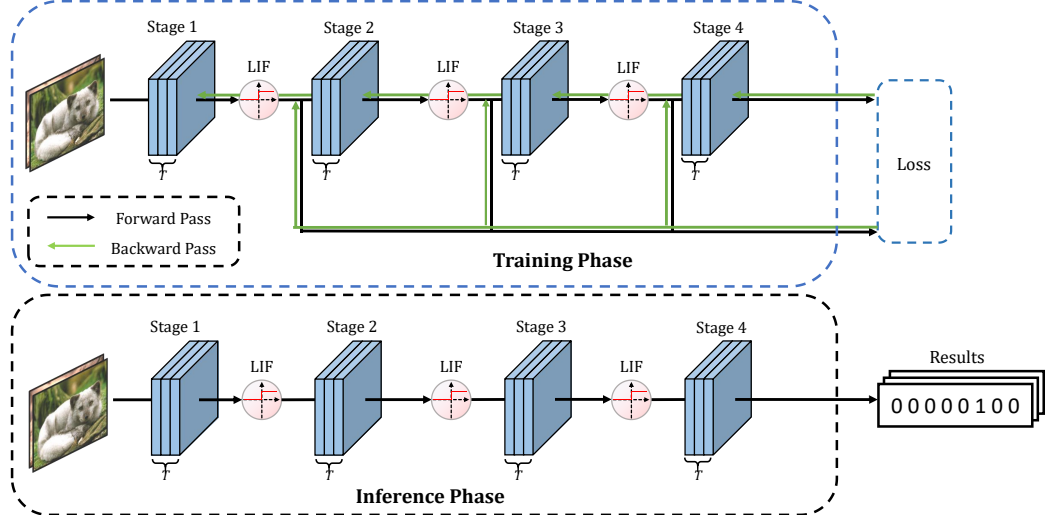


Figure 1: The overall workflow of the proposed method. We add multiple shortcut branches from the intermediate layers to the output thus the gradient from the output could be present to the shallow layers directly.

sigmoid function, the \tanh -like function, and the rectangular function were used as the surrogates respectively in [2], [54], [13], and [5]. However, there is still an intrinsic problem for SG methods, the gradient vanishing, that since the firing function is a bounded function, all these surrogate functions are bounded too, whose gradient would be or close to 0 in most intervals, thus the gradient of the SNN would be reduced quickly as it passes from output to input, which would result in the weights of the shallow layers of the SNN just freezing in the optimization. We will theoretically and experimentally show the gradient vanishing problem in Sec. 4.1.

To handle this problem, we advocate transmitting the gradient from the loss to the shallow layers directly and propose a shortcut back-propagation method in the paper. Specifically, we add multiple shortcut branches from the intermediate layers to the output in the network thus the information from the shallow layers could directly reach the output and then the final loss. In this manner, the gradient from output would be present to the shallow layers directly, thus the weights of the shallow layers would be updated adequately, which will benefit the accuracy. Moreover, these shortcut branches could be removed and will not introduce any burden in the inference phase. Since each shortcut branch will generate a result, the proposed training framework can be seen as a joint optimization problem on the weighted sum of the loss functions associated with these shortcut branches. If we give more weight to the main branch net, the earlier layer weights can not be updated sufficiently. While if we give more attention to the side shortcut branches, the accuracy cannot reach a high level, since the accuracy is directly related to the main branch, not the side branch outputs. To better balance the conflict, we propose an evolutionary training framework, where in the early training, we pay more attention to the side branch net and thus weights of shallow layers, in this way, can be updated sufficiently, while at the end of the training, we give more weight to the main branch net, thus the final accuracy can be improved further. We realize this by inducing a balanced coefficient, which changes dynamically with the training epoch. The workflow of our method is shown in Fig. 1.

Our main contributions can be concluded as follows:

- We find that the gradient vanishing problem is very serious for the SNNs with theoretical justifications and in-depth experimental analysis and propose the shortcut back-propagation approach, a simple yet effective method for mitigating the problem. Furthermore, it will not introduce any burden in the inference phase.
- We also propose an evolutionary training framework that can well balance the weights of these branches with a gradual strategy.

- We evaluate our methods on both static (CIFAR-10 [28], CIFAR-100 [28], ImageNet [8]) and spiking (CIFAR10-DVS [31]) datasets with widely used backbones. Results show that the SNN trained with the proposed method is highly effective and efficient.

2 Related Work

2.1 Learning of Spiking Neural Networks

Unsupervised learning [10; 21], converting ANN to SNN (ANN2SNN) [44; 22; 23], and supervised learning [33; 15] are three kinds of commonly used learning paradigms for SNNs. They adopt different strategies to obtain the final well-performance SNN. For the unsupervised learning method, it uses the spike-timing-dependent plasticity (STDP) approach [34] to update the SNN model, which is seen as more biologically plausible. However, due to a lack of clear task supervisory information, this kind of method is usually limited to small-scale networks and datasets yet. The ANN-SNN conversion method [19; 32; 4; 24; 3; 22; 30] trains an ANN first and then converts the ANN to a homogeneous SNN by reusing the trained weights and replacing the ReLU neuron of the ANN with a temporal spiking neuron for the SNN. This kind of method cannot be used for neuromorphic datasets since the ReLU neuron of the ANN cannot hold the rich temporal dynamic behaviors for sequential information. Supervised learning [11; 47] adopts an alternative function to replace the firing process when doing back-propagation, thus the SNN can be trained directly as an ANN. Thanks to the success of the gradient-based optimization approach, it can perform well with only a few time steps on large-scale datasets. Furthermore, this kind of method can handle temporal data too. Benefiting from so many advantages, the supervised learning of the SNN has received increasing interest recently. Our work also belongs to this field.

2.2 Relieving training difficulties for supervised learning of SNNs

As aforementioned, the SG approach is widely used for solving the non-differentiability of SNNs, e.g., the truncated quadratic function [2], the sigmoid function [54], the tanh-like function [13], and the rectangular function [5]. Though the SG method works well usually, it will also induce some other problems. First, there exists a gradient mismatch between the true gradient and the surrogate gradient, which will lead to a slow convergence and poor accuracy. To solve the problem, IM-Loss[13] proposed a dynamic manual SG method, which changes along with epochs to ensure sufficient weight updates and accurate gradients at the same time. Unlike this manual design, the Differentiable Spike method[33] and the differentiable SG search method find the optimal gradient estimation based on a finite difference technique and NAS technique respectively. Second, due to the firing function being a bounded function, all these SG functions are bounded too, thus the gradient would be or close to 0 in most intervals, which makes the gradient vanishing problem very severe in the SNNs. To solve the problem, SEW-ResNet [11] and MS-ResNet [26] advised using the ResNet with activation before addition form and the ResNet with pre-activation form respectively. There are also some works using normalization techniques to handle the vanishing/explosion gradient problems. For example, Threshold-dependent batch normalization (tdBN) [56] normalized the data along the channel dimension and temporal dimension samely. The temporal Batch Normalization Through Time (BNTT), postsynaptic potential normalization (PSP-BN), and temporal effective batch normalization (TEBN) argued that the spike distributions of different timesteps vary wildly and regulated the spike flows by utilizing the separate timestep batch normalization. MPBN [17] added another batch normalization after the membrane potential updating function to justify the data flow again. Similar to batch normalization, using the regularization loss can also mitigate the gradient explosion/vanishing problem. In RecDis-SNN [15], to regulate the spike flow in an appropriate range, a membrane potential regularization loss was proposed. In Spiking PointNet [43], a trained-less but learning-more paradigm was proposed. This method can be seen as using a small network in the training to mitigate the training difficulty problem.

However, all these methods still need to present the gradient from the output layer to the first layer step by step, thus the gradient vanishing problem cannot be solved completely. In this paper, we propose a shortcut back-propagation method. Different from the above methods, we present the gradient from the output layer to these shallow layers directly, thus the gradient vanishing problem can be solved totally.

3 Preliminary

The fundamental and special computing unit of SNNs is the brain-inspired spiking neuron. We use the common spiking Leaky-Integrate-and-Fire (LIF) neuron model in the paper. It is described by the interaction of the membrane potential and input current to mimic the behavior of the brain neuron. To show the spiking neuron in detail, we introduce the notation first. Throughout the paper, we denote the vectors in bold italic letters. For instance, we use the \mathbf{x} and \mathbf{o} to represent the input and target output variables. We denote the matrices or tensors by bold capital letters (e.g., \mathbf{W} is for weights). We denote the constants by small upright or downright letters. For example, $\mathbf{u}_i^{(t)}$ means the i -th membrane potential at time step t . Then, the LIF neuron can be described as follows:

$$\mathbf{u}^{(t+1),\text{pre}} = \tau \mathbf{u}^{(t)} + \mathbf{c}^{(t+1)}, \text{ where } \mathbf{c}^{(t+1)} = \mathbf{W} \mathbf{x}^{(t+1)}, \quad (1)$$

where τ is a constant within $(0, 1)$, which controls the leakage of membrane potential. When τ is 1, the neuron will degenerate to the Integrate-and-Fire (IF) neuron model. $\mathbf{u}^{(t+1),\text{pre}}$ is the pre-synaptic input at time step $t + 1$, which is charged by the input current $\mathbf{c}^{(t+1)}$. Note that we omit the layer index for simplicity. The input current is computed by the dot-product between the weights, \mathbf{W} of the current layer and the spike output, $\mathbf{x}^{(t+1)}$ from the previous layer. Once the membrane potential, $\mathbf{u}^{(t+1),\text{pre}}$ exceeds the firing threshold V_{th} , a spike will be fired from the LIF neuron, given by

$$\mathbf{o}^{(t+1)} = \begin{cases} 1 & \text{if } \mathbf{u}^{(t+1),\text{pre}} > V_{\text{th}}, \\ 0 & \text{otherwise} \end{cases}, \quad \mathbf{u}^{(t+1)} = \mathbf{u}^{(t+1),\text{pre}} \cdot (1 - \mathbf{o}^{(t+1)}) \quad (2)$$

After firing, the spike output $\mathbf{o}^{(t+1)}$ will propagate to the next layer and become the input $\mathbf{x}^{(t+1)}$ of the next layer.

There is a notorious problem in SNN training the firing function is undifferentiable. To demonstrate this problem, we formulate the gradient by the chain rule, given as

$$\frac{\partial L}{\partial \mathbf{W}} = \sum_t \left(\frac{\partial L}{\partial \mathbf{o}^{(t)}} \frac{\partial \mathbf{o}^{(t)}}{\partial \mathbf{u}^{(t),\text{pre}}} + \frac{\partial L}{\partial \mathbf{u}^{(t+1),\text{pre}}} \frac{\partial \mathbf{u}^{(t+1),\text{pre}}}{\partial \mathbf{u}^{(t),\text{pre}}} \right) \frac{\partial \mathbf{u}^{(t),\text{pre}}}{\partial \mathbf{W}}. \quad (3)$$

Since the firing function (Eq. (2)) is similar to the sign function. The $\frac{\partial \mathbf{o}^{(t)}}{\partial \mathbf{u}^{(t),\text{pre}}}$ is 0 almost everywhere except for the threshold. Therefore, the updates for weights would either be 0 or infinity if we use the actual gradient of the firing function.

4 Methodology

4.1 The Gradient Vanishing Problem for SNNs

As aforementioned, the non-differentiability of SNNs make it difficult to train the SNNs directly. To mitigate this problem, the surrogate gradient was proposed. In this kind of method, the firing function remains the same when performing the forward pass, while, becomes a surrogate function when performing the backward pass. Then the surrogate gradient can be computed by the the surrogate function. Three popular surrogate gradients are

$$\begin{cases} \frac{\partial \mathbf{o}^{(t)}}{\partial \mathbf{u}^{(t),\text{pre}}} = \gamma \max \left(0, 1 - \left| \frac{\mathbf{u}^{(t),\text{pre}}}{V_{\text{th}}} - 1 \right| \right), \\ \frac{\partial \mathbf{o}^{(t)}}{\partial \mathbf{u}^{(t),\text{pre}}} = \frac{1}{a} \text{sign} \left(\left| \mathbf{u}^{(t),\text{pre}} - V_{\text{th}} \right| < \frac{a}{2} \right), \\ \frac{\partial \mathbf{o}^{(t)}}{\partial \mathbf{u}^{(t),\text{pre}}} = k(1 - \tanh(\mathbf{u}^{(t),\text{pre}} - V_{\text{th}}))^2. \end{cases} \quad (4)$$

All of them have a hyper-parameter to control the sharpness and the width of the surrogate gradient. However, it can be seen that these gradients would be or close to 0 in most intervals, which will cause a severe gradient vanishing problem. Though the residual block can reduce the gradient vanishing problem effectively, it does not work well for SNNs. To show this, we formulate the skip connection by

$$\mathbf{o} = g(f(\mathbf{x}) + \mathbf{x}), \quad (5)$$

where $f(\cdot)$ is the convolutional layers and activation layers in the main path, and $g(\cdot)$ is the activation function. In ANNs, the $g(\cdot)$ is ReLU. Since ReLU is unbounded for the positive part, the gradient can be passed to the input of the block. In the case of SNNs, the $g(\cdot)$ is LIF and the gradient will be reduced through the surrogate gradient, thus causing the gradient vanishing problem.

4.2 The Shortcut Back-propagation Method

Both theoretical analysis and experiments show that the gradient vanishing problem is severe. To solve the problem, we first propose a shortcut back-propagation method in the paper. In specific, the network can be divided into several blocks commonly. We add multiple shortcut branches from these blocks to the output directly shown in Fig. 1, These blocks are followed right with a global average pooling layer and a fully connected layer, thus the final output will become

$$\mathbf{o}_{\text{final}} = \sum_l b_l(\mathbf{x}), \quad (6)$$

where the $b_l(\mathbf{x})$ represents the output of the l -th block. While the original final output is

$$\mathbf{o}_{\text{final}} = b_n(\mathbf{x}), \text{ where } b_l(\mathbf{x}) = f_l(b_{l-1}(\mathbf{x})). \quad (7)$$

In the above equation, the n is the total number of the blocks and $f_l(\cdot)$ is the network of the l -th block. To show how can our method mitigate the gradient vanishing problem, we take the gradient of the weight of the first layer as an example. For the original case, it is

$$\frac{\partial L}{\partial \mathbf{W}_1} = \frac{\partial L}{\partial b_n(\mathbf{x})} \frac{\partial b_n(\mathbf{x})}{\partial b_{n-1}(\mathbf{x})} \dots \frac{\partial b_{l+1}(\mathbf{x})}{\partial b_l(\mathbf{x})} \frac{\partial b_l(\mathbf{x})}{\partial \mathbf{W}_1}. \quad (8)$$

Since the $\frac{\partial b_{l+1}(\mathbf{x})}{\partial b_l(\mathbf{x})}$ is always reduced through the surrogate gradient, the $\frac{\partial L}{\partial \mathbf{W}_1}$ will be very small and the weight cannot be updated sufficiently. However, for our method, it is

$$\frac{\partial L}{\partial \mathbf{W}_1} = \sum_l \frac{\partial L}{\partial b_l(\mathbf{x})} \frac{\partial b_l(\mathbf{x})}{\partial \mathbf{W}_1}. \quad (9)$$

In our method, the gradient will be presented to the first block directly and then the \mathbf{W}_1 . Thus the gradient vanishing problem can be solved completely. To further illustrate this advantage, we visualize the gradient distribution of the first layer for Spiking ResNet20 on the CIFAR 10 in the ???. It can be seen that the distribution is relatively flat, meaning the gradient vanishing problem has been well solved for these shallow layers. What's more, these shortcut branches can be removed in the inference time, thus introducing no extra cost.

4.3 The Evolutionary Training Framework

Though the shortcut back-propagation method can mitigate the gradient vanishing problem well, it would induce a conflict. Every shortcut will generate a result to the final output. If we pay more attention to these outputs from the shallow layers, the final result cannot lead to high accuracy, since these shortcut branches will be removed in the inference phase and the final accuracy is only related to the main branch. However, if we give more weight to the output from the main branch, the final loss can not take enough information from these shallow layers and, therefore, can not drive the update of weights of these shallow layers sufficiently.

To solve the problem, we propose an evolutionary training framework. In the early training, we pay more attention to the former side branch net, and thus weights of shallow layers can be updated sufficiently. Then we gradually pay more attention to the main branch net until all attention to the main net at the end of the training. In this way, the final accuracy can be improved further. We introduce a balance coefficient, $\lambda(i)$ and adopt a strategy of decreasing to adjust it as follows,

$$\mathbf{o}_{\text{final}} = b_n(\mathbf{x}) + \lambda(i) \sum_{l=1}^I b_l(\mathbf{x}), \text{ where } \lambda(i) = \lambda(1 - \frac{i}{I}). \quad (10)$$

In the above equation, I is the total number of the training iterations, i is the current training iteration, and λ is a constant. We set λ as 0.25 in the work.

The training and inference of our SNN are detailed in Algo. 1.

5 Experiment

In this section, we conduct extensive experiments on CIFAR-10(100) [28], ImageNet [8], and CIFAR10-DVS [31] to demonstrate the superior performance of our method. The CIFAR-10(100)

Algorithm 1 Training and inference procedure of SNN with our method.

Training

Input: An SNN to be trained; Initial balance coefficient λ ; training dataset; total training iteration: I_{train} .

Output: The well-trained SNN.

- 1: **for** all $i = 1, 2, \dots, I_{\text{train}}$ iteration **do**
- 2: Get mini-batch training data, $\mathbf{x}_{\text{in}}(i)$ and class label, $\mathbf{y}(i)$;
- 3: Feed the $\mathbf{x}_{\text{in}}(i)$ into the SNN and calculate every block output $b_l(\mathbf{x}_{\text{in}}(i))$ and the final main net output $b_n(\mathbf{x}_{\text{in}}(i))$;
- 4: Update λ ;
- 5: Calculate the final output by Eq. 10;
- 6: Compute classification loss $L_{\text{CE}} = \mathcal{L}_{\text{CE}}(\mathbf{o}_{\text{final}}(i), \mathbf{y}(i))$;
- 7: Calculate the gradient w.r.t. \mathbf{W} by Eq. 9;
- 8: Update \mathbf{W} : $(\mathbf{W} \leftarrow \mathbf{W} - \eta \frac{\partial L}{\partial \mathbf{W}})$ where η is learning rate.
- 9: **end for**

Inference

Input: The trained SNN; test dataset; total test iteration: I_{test} .

Output: The classification result.

- 1: **for** all $i = 1, 2, \dots, I_{\text{test}}$ iteration **do**
- 2: Get mini-batch test data, $\mathbf{x}_{\text{in}}(i)$ and class label, $\mathbf{y}(i)$ in test dataset;
- 3: Feed the $\mathbf{x}_{\text{in}}(i)$ into the trained SNN;
- 4: Calculate the final main net output $b_n(\mathbf{x}_{\text{in}}(i))$;
- 5: Calculate the final output, $\mathbf{o}_{\text{final}}(i) = b_n(\mathbf{x}_{\text{in}}(i))$;
- 6: Compare the final output $\mathbf{o}_{\text{final}}(i)$ and $\mathbf{y}(i)$ to compute the classification result.
- 7: **end for**

Table 1: Ablation study for the shortcut back-propagation method.

Dataset	Architecture	Method	Time-step	Accuracy
ResNet18		Vanilla Training	2	71.42%
		Shortcut Back-propagation	2	73.68%
		Evolutionary Training	2	74.02%
		Vanilla Training	4	72.22%
		Shortcut Back-propagation	4	74.78%
		Evolutionary Training	4	74.83%
CIFAR-100		Vanilla Training	2	69.82%
		Shortcut Back-propagation	2	74.06%
		Evolutionary Training	2	74.17%
		Vanilla Training	4	69.98%
		Shortcut Back-propagation	4	75.67%
		Evolutionary Training	4	75.81%

dataset consists of 50k training images and 10k test images in 10(100) classes with 32×32 pixels. The CIFAR10-DVS dataset is converted by the CIFAR-10 dataset and composed of 10k images in 10 classes, with 1k images per class. ImageNet is a relatively large dataset that has more than 1,250k training images and 50k test images. For these static datasets (CIFAR-10, CIFAR-100, and ImageNet), we applied data normalization to ensure that they have 0 mean and 1 variance. To avoid overfitting, we also conducted random horizontal flipping and cropping on all these datasets. For a fair comparison, AutoAugment [6] was also used for data augmentation following these work [14; 33] on CIFAR-10(100). For the static dataset, CIFAR10-DVS, we split it into 9k training images and 1k test images following to [48] first and resized the training image frames to 48×48 as in [56]. We also adopted random horizontal flip and random roll within 5 pixels. While for the test images, we just resized them to 48×48 without any additional processing as in [33].

Table 2: Comparison with SoTA methods on CIFAR-10(100).

Dataset	Method	Type	Architecture	Timestep	Accuracy
CIFAR-10	SpikeNorm [44]	ANN2SNN	VGG16	2500	91.55%
	Hybrid-Train [42]	Hybrid training	VGG16	200	92.02%
	TSSL-BP [55]	SNN training	CIFARNet	5	91.41%
	TL [45]	Tandem Learning	CIFARNet	8	89.04%
	PTL [46]	Tandem Learning	VGG11	16	91.24%
	PLIF [12]	SNN training	PLIFNet	8	93.50%
	DSR [36]	SNN training	ResNet18	20	95.40%
	KDSNN [51]	SNN training	ResNet18	4	93.41%
	Diet-SNN [41]	SNN training	ResNet20	5	91.78%
				10	92.54%
	Dspike [33]	SNN training	ResNet20	2	93.13%
				4	93.66%
CIFAR-100	STBP-tdBN [56]	SNN training	ResNet19	2	92.34%
				4	92.92%
	TET [9]	SNN training	ResNet19	2	94.16%
				4	94.44%
	RecDis-SNN [15]	SNN training	ResNet19	2	93.64%
				4	95.53%
	Real Spike [16]	SNN training	ResNet19	2	95.31%
				4	95.51%
			ResNet20	4	91.89%
	Shortcut Back-propagation	SNN training	ResNet18	1	93.89% \pm 0.11
				2	93.92% \pm 0.08
CIFAR-100	Evolutionary Training	SNN training	ResNet18	2	94.30% \pm 0.09
				4	94.46% \pm 0.11
	RMP [20]	ANN2SNN	ResNet20	2048	67.82%
	Hybrid-Train [42]	Hybrid training	VGG11	125	67.90%
	T2FSNN [38]	ANN2SNN	VGG16	680	68.80%
	Real Spike [16]	SNN training	ResNet20	5	66.60%
	LTL [52]	Tandem Learning	ResNet20	31	76.08%
	Diet-SNN [41]	SNN training	ResNet20	5	64.07%
	RecDis-SNN [15]	SNN training	ResNet19	4	74.10%
	Dspike [33]	SNN training	ResNet20	2	71.68%
				4	73.35%
	TET [9]	SNN training	ResNet19	2	72.87%
				4	74.47%
Shortcut Back-propagation	SNN training	ResNet18	2	73.68% \pm 0.10	
			4	74.02% \pm 0.08	
	Evolutionary Training	SNN training	ResNet18	2	74.78% \pm 0.09
			4	74.83% \pm 0.11	

5.1 Ablation Study

To validate the effectiveness of the proposed shortcut back-propagation method, we initially conducted several ablation experiments on the CIFAR-100 dataset using ResNet18 and ResNet34 with different timesteps. The results are detailed in Tab. 1. For ResNet18, the accuracy achieved through vanilla training is 71.42% and 72.22% under 2 and 4 timesteps, respectively, which aligns with existing works. Upon applying our shortcut back-propagation method, the accuracy improved to 73.68% and 74.78%, marking a notable 2.5% enhancement. Furthermore, with the evolutionary training method, the performance of ResNet18 saw an additional improvement, reaching 74.02% and 74.83%, respectively. Under vanilla training, ResNet34 achieved accuracies of 69.82% and 69.98% with 2 and 4 timesteps, respectively. These results are actually worse than those obtained with ResNet18. This suggests that the deeper model does not exhibit better performance due to the significant gradient vanishing problem in SNNs. However, by utilizing our shortcut back-propagation method, the accuracy significantly improves to 74.06% and 75.67%, representing a remarkable 5.0% enhancement. Notably, these results surpass the performance of ResNet18 as well. This clearly demonstrates the effectiveness of our proposed method. Furthermore, when incorporating the evolutionary training method, we observe

further improvements in performance. In summary, our proposed method proves highly effective in substantially enhancing accuracy.

5.2 Comparison with SoTA methods

In this section, we conducted a comparative experiment for the shortcut back-propagation method and the evolutionary training framework, taking into consideration several state-of-the-art works. To ensure a fair comparison, we present the top-1 accuracy results based on 3 independent trials. We first evaluated our method on CIFAR-10 and CIFAR-100 datasets. The results are summarized in Tab. 2. For the CIFAR-10 dataset, we chose SpikeNorm [44], Hybrid-Train [42], TSSL-BP [55], TL [45], PTL [46], PLIF [12], DSR [36], KDSNN [51], Diet-SNN [41], Dspike [33], STBP-tdBN [56], TET [9], RecDis-SNN [15], and Real Spike [16] as our comparison. Previous works utilizing ResNet18, ResNet19, and ResNet20 as backbones achieved the highest accuracies of 95.40%, 95.51%, and 93.66% with 20, 4, and 4 timesteps respectively. While our shortcut back-propagation method based on ResNet18 could reach 93.92. Note that, ResNet18 is smaller than ResNet20. By incorporating the evolutionary training framework, our SNN models exhibit the capability to attain higher levels of accuracy. On the CIFAR-100 dataset, our method using the ResNet18 outperforms the current best method, TET and RecDis-SNN even with ResNet19 by about 0.5%. These experimental results clearly show our method’s efficiency and effectiveness.

Table 3: Comparison with SoTA methods on ImageNet.

Method	Type	Architecture	Timestep	Accuracy
STBP-tdBN [56]	SNN training	ResNet34	6	63.72%
TET [9]	SNN training	ResNet34	6	64.79%
RecDis-SNN [15]	SNN training	ResNet34	6	67.33%
OTTT [49]	SNN training	ResNet34	6	65.15%
GLIF [53]	SNN training	ResNet34	4	67.52%
DSR [36]	SNN training	ResNet18	50	67.74%
MS-ResNet [25]	SNN training	ResNet18	6	63.10%
MPBN [18]	SNN training	ResNet18	4	63.14%
		ResNet34	4	64.71%
Real Spike [16]	SNN training	ResNet18	4	63.68%
		ResNet34	4	67.69%
SEW ResNet [11]	SNN training	ResNet18	4	63.18%
		ResNet34	4	67.04%
Shortcut Back-propagation	SNN training	ResNet18	4	64.47%\pm0.21
		ResNet34	4	67.90%\pm0.17
Evolutionary Training	SNN training	ResNet18	4	65.12%\pm0.18
		ResNet34	4	68.14%\pm0.15

We proceeded to conduct experiments on the ImageNet dataset, which is a more complex dataset than CIFAR. The comparative results are presented in Tab. 3. Notably, there have been several state-of-the-art (SoTA) baselines proposed for this dataset recently, such as RecDis-SNN [15], GLIF [53], DSR [36], MPBN [18], MS-ResNet [25], Real Spike [16], and SEW ResNet [11]. It is important to note that Real Spike and SEW ResNet deviate from the typical ResNet backbone as they generate integer outputs in the intermediate layers, making them more energy-intensive compared to methods with standard backbones. In contrast, our approach adopts the standard ResNet18 and ResNet34 architectures, yet it still outperforms Real Spike and SEW ResNet. Specifically, our method achieves an accuracy of 65.12% and 68.14% using ResNet18 and ResNet34, respectively, surpassing Real Spike by 1.44% and 0.45%, respectively. This improvement is noteworthy and demonstrates the effectiveness of our method in handling large-scale datasets.

In addition to the aforementioned experiments, we conducted tests on the highly popular neuromorphic dataset, CIFAR10-DVS. Employing ResNet18 as the foundational architecture, which is notably smaller compared to ResNet19, our approach achieved remarkable accuracies of 82.00% and 83.30%, respectively. These results not only demonstrate a substantial improvement over previous methodologies but also validate the efficacy of our proposed method.

Table 4: Comparison with SoTA methods on CIFAR10-DVS.

Method	Type	Architecture	Timestep	Accuracy
Rollout [29]	Rollout	DenseNet	10	66.80%
STBP-tdBN [56]	SNN training	ResNet19	10	67.80%
RecDis-SNN [15]	SNN training	ResNet19	10	72.42%
Real Spike [16]	SNN training	ResNet19	10	72.85%
Dspike [33]	SNN training	ResNet18	10	75.40%
Shortcut Back-propagation	SNN training	ResNet18	10	82.00%\pm0.10
Evolutionary Training	SNN training	ResNet18	10	83.30%\pm0.10

6 Conclusion

In the paper, we proved that the Spiking Neural Network suffers severe gradient vanishing with theoretical justifications and in-depth experimental analysis. To mitigate the problem, we proposed a shortcut back-propagation method. This enables us to present the gradient to the shallow layers directly, thereby significantly mitigating the gradient vanishing problem. Additionally, this method does not introduce any burden during the inference phase. we also presented an evolutionary training framework by inducing a balance coefficient that dynamically changes with the training epoch, which could further improve the accuracy. We conducted various experiments to verify the effectiveness of our method.

References

- [1] Akopyan, F., Sawada, J., Cassidy, A., Alvarez-Icaza, R., Arthur, J., Merolla, P., Imam, N., Nakamura, Y., Datta, P., Nam, G.J., et al.: Truenorth: Design and tool flow of a 65 mw 1 million neuron programmable neurosynaptic chip. *IEEE transactions on computer-aided design of integrated circuits and systems* **34**(10), 1537–1557 (2015)
- [2] Bohte, S.M.: Error-backpropagation in networks of fractionally predictive spiking neurons. In: *International Conference on Artificial Neural Networks*. pp. 60–68. Springer (2011)
- [3] Bu, T., Ding, J., Yu, Z., Huang, T.: Optimized potential initialization for low-latency spiking neural networks. In: *Proceedings of the AAAI Conference on Artificial Intelligence*. vol. 36, pp. 11–20 (2022)
- [4] Bu, T., Fang, W., Ding, J., Dai, P., Yu, Z., Huang, T.: Optimal ann-snn conversion for high-accuracy and ultra-low-latency spiking neural networks. In: *International Conference on Learning Representations* (2021)
- [5] Cheng, X., Hao, Y., Xu, J., Xu, B.: Lisnn: Improving spiking neural networks with lateral interactions for robust object recognition. In: *IJCAI*. pp. 1519–1525 (2020)
- [6] Cubuk, E.D., Zoph, B., Mane, D., Vasudevan, V., Le, Q.V.: Autoaugment: Learning augmentation policies from data. *arXiv preprint arXiv:1805.09501* (2018)
- [7] Davies, M., Srinivasa, N., Lin, T.H., Chinya, G., Cao, Y., Choday, S.H., Dimou, G., Joshi, P., Imam, N., Jain, S., et al.: Loihi: A neuromorphic manycore processor with on-chip learning. *Ieee Micro* **38**(1), 82–99 (2018)
- [8] Deng, J., Dong, W., Socher, R., Li, L.J., Li, K., Fei-Fei, L.: Imagenet: A large-scale hierarchical image database. In: *2009 IEEE conference on computer vision and pattern recognition*. pp. 248–255. Ieee (2009)
- [9] Deng, S., Li, Y., Zhang, S., Gu, S.: Temporal efficient training of spiking neural network via gradient re-weighting. *arXiv preprint arXiv:2202.11946* (2022)
- [10] Diehl, P.U., Cook, M.: Unsupervised learning of digit recognition using spike-timing-dependent plasticity. *Frontiers in computational neuroscience* **9**, 99 (2015)
- [11] Fang, W., Yu, Z., Chen, Y., Huang, T., Masquelier, T., Tian, Y.: Deep residual learning in spiking neural networks. *Advances in Neural Information Processing Systems* **34**, 21056–21069 (2021)
- [12] Fang, W., Yu, Z., Chen, Y., Masquelier, T., Huang, T., Tian, Y.: Incorporating learnable membrane time constant to enhance learning of spiking neural networks. In: *Proceedings of the IEEE/CVF International Conference on Computer Vision*. pp. 2661–2671 (2021)

[13] Guo, Y., Chen, Y., Zhang, L., Liu, X., Wang, Y., Huang, X., Ma, Z.: IM-loss: Information maximization loss for spiking neural networks. In: Oh, A.H., Agarwal, A., Belgrave, D., Cho, K. (eds.) *Advances in Neural Information Processing Systems* (2022), https://openreview.net/forum?id=Jw34v_84m2b

[14] Guo, Y., Chen, Y., Zhang, L., Wang, Y., Liu, X., Tong, X., Ou, Y., Huang, X., Ma, Z.: Reducing information loss for spiking neural networks. In: Avidan, S., Brostow, G., Cissé, M., Farinella, G.M., Hassner, T. (eds.) *Computer Vision – ECCV 2022*. pp. 36–52. Springer Nature Switzerland, Cham (2022)

[15] Guo, Y., Tong, X., Chen, Y., Zhang, L., Liu, X., Ma, Z., Huang, X.: Recdis-snn: Rectifying membrane potential distribution for directly training spiking neural networks. In: *Proceedings of the IEEE/CVF Conference on Computer Vision and Pattern Recognition (CVPR)*. pp. 326–335 (June 2022)

[16] Guo, Y., Zhang, L., Chen, Y., Tong, X., Liu, X., Wang, Y., Huang, X., Ma, Z.: Real spike: Learning real-valued spikes for spiking neural networks. In: *Computer Vision–ECCV 2022: 17th European Conference, Tel Aviv, Israel, October 23–27, 2022, Proceedings, Part XII*. pp. 52–68. Springer (2022)

[17] Guo, Y., Zhang, Y., Chen, Y., Peng, W., Liu, X., Zhang, L., Huang, X., Ma, Z.: Membrane potential batch normalization for spiking neural networks. *arXiv preprint arXiv:2308.08359* (2023)

[18] Guo, Y., Zhang, Y., Chen, Y., Peng, W., Liu, X., Zhang, L., Huang, X., Ma, Z.: Membrane potential batch normalization for spiking neural networks. In: *Proceedings of the IEEE/CVF International Conference on Computer Vision (ICCV)*. pp. 19420–19430 (October 2023)

[19] Han, B., Roy, K.: Deep spiking neural network: Energy efficiency through time based coding. In: *European Conference on Computer Vision*. pp. 388–404. Springer (2020)

[20] Han, B., Srinivasan, G., Roy, K.: Rmp-snn: Residual membrane potential neuron for enabling deeper high-accuracy and low-latency spiking neural network. In: *Proceedings of the IEEE/CVF conference on computer vision and pattern recognition*. pp. 13558–13567 (2020)

[21] Hao, Y., Huang, X., Dong, M., Xu, B.: A biologically plausible supervised learning method for spiking neural networks using the symmetric stdp rule. *Neural Networks* **121**, 387–395 (2020)

[22] Hao, Z., Bu, T., Ding, J., Huang, T., Yu, Z.: Reducing ann-snn conversion error through residual membrane potential. *arXiv preprint arXiv:2302.02091* (2023)

[23] Hao, Z., Ding, J., Bu, T., Huang, T., Yu, Z.: Bridging the gap between anns and snns by calibrating offset spikes. *arXiv preprint arXiv:2302.10685* (2023)

[24] Ho, N.D., Chang, I.J.: Tcl: an ann-to-snn conversion with trainable clipping layers. In: *2021 58th ACM/IEEE Design Automation Conference (DAC)*. pp. 793–798. IEEE (2021)

[25] Hu, Y., Deng, L., Wu, Y., Yao, M., Li, G.: Advancing spiking neural networks towards deep residual learning (2023)

[26] Hu, Y., Wu, Y., Deng, L., Li, G.: Advancing residual learning towards powerful deep spiking neural networks. *arXiv preprint arXiv:2112.08954* (2021)

[27] Kim, S., Park, S., Na, B., Yoon, S.: Spiking-yolo: Spiking neural network for energy-efficient object detection (2019)

[28] Krizhevsky, A., Nair, V., Hinton, G.: Cifar-10 (canadian institute for advanced research). URL <http://www.cs.toronto.edu/kriz/cifar.html> **5**(4), 1 (2010)

[29] Kugele, A., Pfeil, T., Pfeiffer, M., Chicca, E.: Efficient processing of spatio-temporal data streams with spiking neural networks. *Frontiers in Neuroscience* **14**, 439 (2020)

[30] Lan, Y., Zhang, Y., Ma, X., Qu, Y., Fu, Y.: Efficient converted spiking neural network for 3d and 2d classification. In: *Proceedings of the IEEE/CVF International Conference on Computer Vision*. pp. 9211–9220 (2023)

[31] Li, H., Liu, H., Ji, X., Li, G., Shi, L.: Cifar10-dvs: an event-stream dataset for object classification. *Frontiers in neuroscience* **11**, 309 (2017)

[32] Li, Y., Deng, S., Dong, X., Gong, R., Gu, S.: A free lunch from ann: Towards efficient, accurate spiking neural networks calibration. In: *International Conference on Machine Learning*. pp. 6316–6325. PMLR (2021)

[33] Li, Y., Guo, Y., Zhang, S., Deng, S., Hai, Y., Gu, S.: Differentiable spike: Rethinking gradient-descent for training spiking neural networks. *Advances in Neural Information Processing Systems* **34**, 23426–23439 (2021)

[34] Lobov, S.A., Mikhaylov, A.N., Kazantsev, V.B.: Spatial properties of stdp in a self-learning spiking neural network enable controlling a mobile robot. *Frontiers in Neuroscience* **14**, – (2020)

[35] Ma, D., Shen, J., Gu, Z., Zhang, M., Zhu, X., Xu, X., Xu, Q., Shen, Y., Pan, G.: Darwin: A neuromorphic hardware co-processor based on spiking neural networks. *Journal of Systems Architecture* **77**, 43–51 (2017)

[36] Meng, Q., Xiao, M., Yan, S., Wang, Y., Lin, Z., Luo, Z.Q.: Training high-performance low-latency spiking neural networks by differentiation on spike representation. In: *Proceedings of the IEEE/CVF Conference on Computer Vision and Pattern Recognition*. pp. 12444–12453 (2022)

[37] Neftci, E.O., Mostafa, H., Zenke, F.: Surrogate gradient learning in spiking neural networks: Bringing the power of gradient-based optimization to spiking neural networks. *IEEE Signal Processing Magazine* **36**(6), 51–63 (2019)

[38] Park, S., Kim, S., Na, B., Yoon, S.: T2fsnn: Deep spiking neural networks with time-to-first-spike coding. In: *2020 57th ACM/IEEE Design Automation Conference (DAC)*. pp. 1–6. IEEE (2020)

[39] Pei, J., Deng, L., Song, S., Zhao, M., Zhang, Y., Wu, S., Wang, G., Zou, Z., Wu, Z., He, W., et al.: Towards artificial general intelligence with hybrid tianjic chip architecture. *Nature* **572**(7767), 106–111 (2019)

[40] Qu, J., Gao, Z., Zhang, T., Lu, Y., Tang, H., Qiao, H.: Spiking neural network for ultra-low-latency and high-accurate object detection (2023)

[41] Rathi, N., Roy, K.: Diet-snn: Direct input encoding with leakage and threshold optimization in deep spiking neural networks. *arXiv preprint arXiv:2008.03658* (2020)

[42] Rathi, N., Srinivasan, G., Panda, P., Roy, K.: Enabling deep spiking neural networks with hybrid conversion and spike timing dependent backpropagation. *arXiv preprint arXiv:2005.01807* (2020)

[43] Ren, D., Ma, Z., Chen, Y., Peng, W., Liu, X., Zhang, Y., Guo, Y.: Spiking pointnet: Spiking neural networks for point clouds. *arXiv preprint arXiv:2310.06232* (2023)

[44] Sengupta, A., Ye, Y., Wang, R., Liu, C., Roy, K.: Going deeper in spiking neural networks: Vgg and residual architectures. *Frontiers in neuroscience* **13**, 95 (2019)

[45] Wu, J., Chua, Y., Zhang, M., Li, G., Li, H., Tan, K.C.: A tandem learning rule for effective training and rapid inference of deep spiking neural networks. *IEEE Transactions on Neural Networks and Learning Systems* (2021)

[46] Wu, J., Xu, C., Han, X., Zhou, D., Zhang, M., Li, H., Tan, K.C.: Progressive tandem learning for pattern recognition with deep spiking neural networks. *IEEE Transactions on Pattern Analysis and Machine Intelligence* **44**(11), 7824–7840 (2021)

[47] Wu, Y., Deng, L., Li, G., Zhu, J., Shi, L.: Spatio-temporal backpropagation for training high-performance spiking neural networks. *Frontiers in neuroscience* **12**, 331 (2018)

[48] Wu, Y., Deng, L., Li, G., Zhu, J., Xie, Y., Shi, L.: Direct training for spiking neural networks: Faster, larger, better. In: *Proceedings of the AAAI Conference on Artificial Intelligence*. vol. 33, pp. 1311–1318 (2019)

[49] Xiao, M., Meng, Q., Zhang, Z., He, D., Lin, Z.: Online training through time for spiking neural networks. In: Oh, A.H., Agarwal, A., Belgrave, D., Cho, K. (eds.) *Advances in Neural Information Processing Systems* (2022), <https://openreview.net/forum?id=Siv3nHYHheI>

[50] Xiao, M., Meng, Q., Zhang, Z., Wang, Y., Lin, Z.: Training feedback spiking neural networks by implicit differentiation on the equilibrium state. *Advances in Neural Information Processing Systems* **34**, 14516–14528 (2021)

[51] Xu, Q., Li, Y., Shen, J., Liu, J.K., Tang, H., Pan, G.: Constructing deep spiking neural networks from artificial neural networks with knowledge distillation. *arXiv preprint arXiv:2304.05627* (2023)

[52] Yang, Q., Wu, J., Zhang, M., Chua, Y., Wang, X., Li, H.: Training spiking neural networks with local tandem learning. *arXiv preprint arXiv:2210.04532* (2022)

[53] Yao, X., Li, F., Mo, Z., Cheng, J.: Glif: A unified gated leaky integrate-and-fire neuron for spiking neural networks. *arXiv preprint arXiv:2210.13768* (2022)

- [54] Zenke, F., Ganguli, S.: Superspike: Supervised learning in multilayer spiking neural networks. *Neural computation* **30**(6), 1514–1541 (2018)
- [55] Zhang, W., Li, P.: Temporal spike sequence learning via backpropagation for deep spiking neural networks. *Advances in Neural Information Processing Systems* **33**, 12022–12033 (2020)
- [56] Zheng, H., Wu, Y., Deng, L., Hu, Y., Li, G.: Going deeper with directly-trained larger spiking neural networks. In: *Proceedings of the AAAI Conference on Artificial Intelligence*. vol. 35, pp. 11062–11070 (2021)
- [57] Zou, S., Mu, Y., Zuo, X., Wang, S., Cheng, L.: Event-based human pose tracking by spiking spatiotemporal transformer (2023)